frontiers | Frontiers in Chemical Engineering

TYPE Original Research
PUBLISHED 03 October 2024
DOI 10.3389/fceng.2024.1479798

OPEN ACCESS

EDITED BY
Mohammad Tavakkoli Yaraki,
Macquarie University, Australia

REVIEWED BY
Narges Elmi Fard,
Islamic Azad University, Iran
Marzieh Ramezani Farani,
Inha University, Republic of Korea
Iman Akbarzadeh,
Sharif University of Technology, Iran

*CORRESPONDENCE
Heejoon Park,
hpark4@una.edu

RECEIVED 12 August 2024
ACCEPTED 26 September 2024
PUBLISHED 03 October 2024

CITATION
Park H and Johnson PA (2024) The development and evaluation of chitosan-coated enzyme magnetic nanoparticles for cellulose hydrolysis.
Front. Chem. Eng. 6:1479798.
doi: 10.3389/fceng.2024.1479798

The development and evaluation of chitosan-coated enzyme magnetic nanoparticles for cellulose hydrolysis

Heejoon Park[1]* and Patrick A. Johnson[2]

[1]Department of Engineering and Industrial Professions, University of North Alabama, Florence, AL, United States, [2]Department of Materials Science and Engineering, Iowa State University, Ames, IW, United States

The recycling capability, colloidal and thermal stability of exo-cellulase, endo-cellulase, and β-glucosidases with magnetic particles (MNPs) were evaluated. Co-precipitation and oxidation of $Fe(OH)_2$ methods were used to fabricate magnetic nanoparticles. Three different enzymes were covalently bound to the surface of MNPs using 3-(aminopropyl) triethoxysilane (APTES) and a common protein crosslinking agent, glutaraldehyde. To evaluate the increase in colloidal dispersion stability, chitosan-coating was applied on MNPs and evaluated through particle settlement tests. The results showed that the chitosan-coated MNPs had 3.7 times higher colloidal dispersion stability than the bare MNPs. X-ray photoelectron spectroscopy (XPS) confirmed each magnetic nanoparticle surface modification step and successful enzyme binding. The optimum bioconjugate ratio in exo-cellulase, endo-cellulase, and β-glucosidases was evaluated, and having a high endo-cellulase bioconjugate in the reaction produced the highest glucose. The bioconjugates showed superior glucose productivity 39.4% at 65°C and 22.2% at 88°C in which the native enzyme is inactivated completely after 5 h of exposure. Recycling stability studies showed approximately 78% of activity was retained after 10 cycles and 32% of activity was retained after 20 cycles. The bioconjugates demonstrated equivalent total product conversions as a single reaction of an equivalent amount of the native enzyme after the 10th cycle this work introduces a novel method for covalently binding individual exo-cellulase, endo-cellulase, and β-glucosidases. These bioconjugates showed superior thermal stability and recyclability. It was also demonstrated that chitosan coating significantly improves the colloidal dispersion stability of bioconjugates. Thus this work validates the use of enzyme-MNP bioconjugates to effectively glucose production and promising technique for eventual continuous biological processes.

KEYWORDS

cellulase, biofuel, enzyme, magnetic nanoparticles (MNP), chitosan

1 Introduction

Increased attention has been given to a new promising source of sugars that could also be converted into biofuels or other chemicals and the global challenge for biorefineries is to use biomass cost-effectively through biological processes. A key issue in biorefineries is the enzymatic hydrolysis of the biomass into fermentable sugars (Michelin et al., 2020; Gomes et al., 2021). Endo cellulase, exco cellulase and β-glucosidases are a group of enzymes that

function together to break down cellulose. Challenges in enzymatic hydrolysis include the varying composition of feedstock and the instability and high cost of the enzymes (Pino et al., 2019). Despite these challenges, enzymatic hydrolysis offers advantages over acid hydrolysis, such as lower energy consumption and no risk of equipment corrosion (Barbosa et al., 2020). The research of enzymatic hydrolysis is considered as vital area, not only from a biological perspective but also from economic and environmental viewpoints. Techno-economic analyses reported in the literature highlight that cellulolytic enzymes account for a substantial portion of production costs, which is a key factor influencing the final price of ethanol (Liu et al., 2016; van Rijn et al., 2018; Larnaudie et al., 2019). The cost of enzymes accounts for approximately 15% of the total expenses of a biorefinery, making it the second largest after feedstock. Additionally, life cycle assessment studies indicate that enzyme dosage in the biorefinery process significantly influences the global warming impact (GWI) (Himmel et al., 2007; Wen et al., 2009; Papadaskalopoulou et al., 2019) These impacts and costs can be minimized by increasing the use of enzymes or implementing recycling processes. Research on the economic feasibility of incorporating a cellulase recycling system in bioethanol production has shown promising financial outcomes (Gomes et al., 2015; Gomes et al., 2018; Gomes et al., 2021).

Recent research has shown that enzymes or drug molecules can be effectively immobilized or carried on various solid supports, such as polymer (Godjevargova et al., 1999; KUMAR, 2000; Amorim et al., 2003).magnetic oxide (Paz-Cedeno et al., 2021), nanotubes (Sillu and Agnihotri, 2020), and porous biochar (Mo et al., 2020). Among these, nanosized magnetic oxide has been drawing attention due to its versatility and unique magnetic properties and applied in various areas such as the food industry (Elmi Fard and Fazaeli, 2022; Dong et al., 2024) biomedical and environmental applications (Horák et al., 2007; Zahn et al., 2020; Ramezani Farani et al., 2022; Vandani et al., 2023; Rezaei et al., 2024; Verma et al., 2024), tissue engineering (Baniasadi et al., 2015), and magnetic resonance imaging (Gossuin et al., 2022; Mohandes et al., 2022). These magnetic nanoparticle supports offer the advantage of easy separation and enzyme recycling capability through the application of an external magnetic field. Additionally, this separation method does not interfere with the medium, reducing the risk of contamination. However, there are still unresolved issues regarding the immobilization of enzymes on magnetic supports, particularly nanoparticle aggregates (Gossuin et al., 2022; Nedylakova et al., 2024) and the effects on the enzyme activity during the harsh process, and the challenges of applying this technology to real substrates (Gomes et al., 2021) Therefore, the study and use of immobilized enzymes on magnetic nanoparticles (MNPs) are crucial for advancing these valorization biological processes, with potential to influence other processes based on cellulosic biomass.

In this study, we explored the enhancement of colloidal stability in magnetic nanoparticles to prevent particle aggregates through surface modification using chitosan. Chitosan is a linear copolymer obtained through the deacetylation of chitin. It consists of varying molar fractions of d-glucosamine and N-acetyl glucosamine units that are randomly arranged along the polysaccharide chain (Neeraj et al., 2016; Matusiak et al., 2022). This chemical structure enables easy functionalization, offering a wide variety of applications for chitosan, such as the production of wound dressings, artificial skin, and cosmetics (Ravi Kumar, 2000), The presence of a large number of amino and hydroxyl groups allows chitosan to form a macroscopic phase of the polymer-surfactant complexes which can stabilize the colloidal system (Guzmán et al., 2016). In this study, we also investigated the immobilization of individual exo-cellulase, endo-cellulase, and β-glucosidases separately on the MNP surface. Many studies have explored the immobilization of cellulase enzymes using a cellulase complex mixture, commonly known as a cocktail (Garcia et al., 1989; Paljevac et al., 2007; Mo et al., 2020; Sillu and Agnihotri, 2020; Paz-Cedeno et al., 2021; Zanuso et al., 2022). The cellulase complex consists of enzymes that break down cellulose into glucose units. These enzymes include endo-cellulase, exo-cellulase, and β-glucosidases. However, due to the random immobilization of these enzymes on solid supports, the activity retention and overall efficiency can vary. There has been limited investigation into the immobilization of individual enzymes to determine which one plays the most crucial role in glucose production from cellulosic material. We also assessed the impact of hydrolysis with various ratios of endo-cellulase, exo-cellulase, and β-glucosidases bioconjugates on carboxyl methylcellulose and pretreated cellulose by measuring glucose production. We have investigated recycling stability over 20 cycles. and thermal stability at 45°C, 65°C and 85 C

2 Experiments

2.1 Materials

β-glucosidase from Aspergillus niger was kindly provided by Novozyme (Bagsvaerd, Denmark). Exo-cellulase and Endo-cellulase from *Trichoderma longibrachiatum* were acquired from Megazyme (Wicklow, Ireland). 3-(aminopropyl) triethoxysilane (APTES) (99%), iron (II) chloride, glutaraldehyde (8%, v/v, aqueous), cellobiose, carboxymethyl cellulose (CMC), chitosan (medium molecular weight), sodium tripolyphosphate (TPP), 3,5-dinitrosalicylic acid, sodium hydroxide, phenol, Rochelle salts (Na-K tartrate), sodium metabisulfite, and citric acid were obtained from Sigma-Aldrich (St. Louis, MO). Hydrogen peroxide (30%, v/v) was sourced from Fisher Scientific (Pittsburgh, PA). Anhydrous methanol (ACS grade) and sodium citrate dihydrate were purchased from EMD Chemicals (Gibbstown, NJ). The protein assay kit (BCS assay) was obtained from Thermo Scientific (Rockford, IL). Neodymium magnets (14,800 G) were procured from K and J Magnetics, Inc (Jamison, PA). Deionized (DI) water (18.2 Ω) was used to prepare aqueous solutions.

2.2 Magnetic nanoparticle fabrication

MNPs were prepared by oxidative alkaline hydrolysis of ferrous ions, which was described in Figure 1 (Park et al., 2011; Park et al., 2018). Briefly, ferrous chloride ($FeCl_2$) was dissolved in 50 mL of deionized water to create a 0.05M $FeCl_2$ solution. To this solution, 1 M potassium hydroxide (KOH) was added to form an aqueous suspension of ferrous hydroxide ($Fe(OH)_2$). The pH of the mixture was carefully adjusted to a range of 7.9–8.0 while continuously

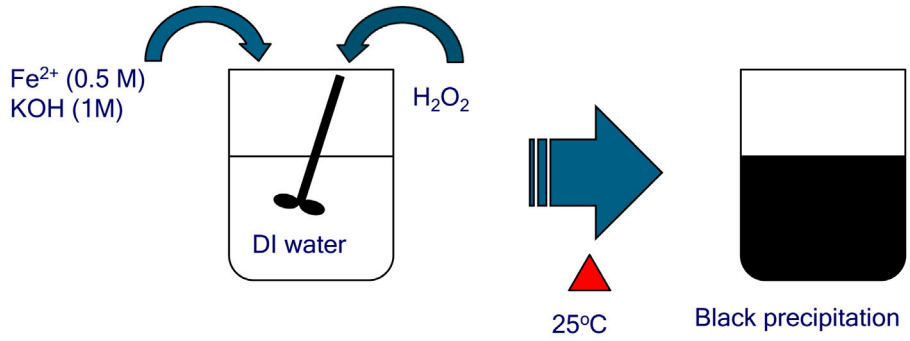

$$Fe^{2+} + \tfrac{1}{2}\,H_2O + \tfrac{1}{4}\,O_2 \rightarrow Fe^{3+} + OH^-$$
$$Fe^{2+} + 2OH^- \rightarrow Fe(OH)_2$$
$$Fe^{3+} + 3OH^- \rightarrow Fe(OH)_3$$
$$Fe(OH)_3 + Fe(OH)_2 + H_2O_2 \rightarrow Fe_3O_4 + \gamma\text{-}Fe_2O_3$$

FIGURE 1
Schematic representation of one-step chemical co-precipitation method for the synthesis of magnetic nanoparticles.

stirring to ensure uniform mixing. The precipitation reaction was allowed to proceed for 2 h at room temperature, resulting in the formation of black precipitates. The separated MNPs were then subjected to a series of washes: three times with 50 mL of deionized water to remove any residual reactants, followed by two washes with 50 mL of ethanol to further purify the nanoparticles. After washing, the MNPs were dried at room temperature to obtain the final product.

2.3 Magnetic nanoparticle surface modification

2.3.1 APTES and glutaraldehyde modification

Using sonication, 10 mg of MNPs were dispersed in 10 mL of a 10% (v/v) APTES solution. The resulting suspension was agitated overnight at room temperature, followed by separation via magnetic decantation. The MNPs underwent three washing cycles with 10 mL of anhydrous methanol and were subsequently modified with APTES by sonication and agitation in 10 mL of 8% (v/v) glutaraldehyde (pH 7.4) for 1 h. The MNPs were then isolated by magnetic decantation, washed three times with 10 mL of 50 mM citrate buffer (pH 5.0), and stored in deionized water at 4°C for subsequent enzyme conjugation.

2.3.2 Chitosan coating and glutaraldehyde modification

Chitosan-coated magnetic nanoparticles were prepared (Shown in Figure 2) as follows: Chitosan (CS) solution (4 mg/mL) was prepared by dissolving medium molecular weight chitosan in 2% (v/v) acetic acid. Next, 10 mg of magnetic nanoparticles (MNPs) were dispersed in 10 mL of the CS solution using ultrasonic agitation for 30 min. Subsequently, 5 mL of sodium tripolyphosphate solution (0.5 mg/mL) was added to the CS-MNP mixture and sonicated for another 30 min. The chitosan-coated MNPs were then recovered from the reaction mixture using a magnet, washed three times with deionized water, and incubated in 10 mL of 8% glutaraldehyde (pH 7.4) for 1 h with shaking. The CS-MNPs were stored at 4°C until further use.

2.4 Particle settlement comparison of MNPs, APTES-MNPs and CS-MNP

Particle sedimentation was assessed over time. A 2 mL solution of MNP, APTES-MNP, and CS-MNP (each at 0.025 mg/mL) was placed in a PMMA cuvette, and optical density at 405 nm was measured over a 2-h period with data collected at 10-min intervals.

2.5 Enzyme immobilization

10 mg of surface-modified MNPs and CS-MNP were redispersed in three different enzyme solutions: exo-cellulase (0.72 mg/mL in citrate buffer at pH 5), endo-cellulase (0.87 mg/mL in citrate buffer at pH 5), and β-glucosidase (0.64 mg/mL in citrate buffer at pH 5). The mixtures were gently shaken overnight to ensure proper interaction between the enzymes and the nanoparticles. After the incubation period, the resulting enzyme-MNP bioconjugates were separated from the solution using magnetic decantation. These bioconjugates were then washed three times with 10 mL of citrate buffer to remove any unbound enzymes. After washing, the bioconjugates were redispersed in 10 mL of citrate buffer and stored at 4°C to preserve their stability. The amount of protein (enzyme) that was loaded onto the nanoparticles' surface was determined by analyzing the supernatant from each bioconjugate preparation.

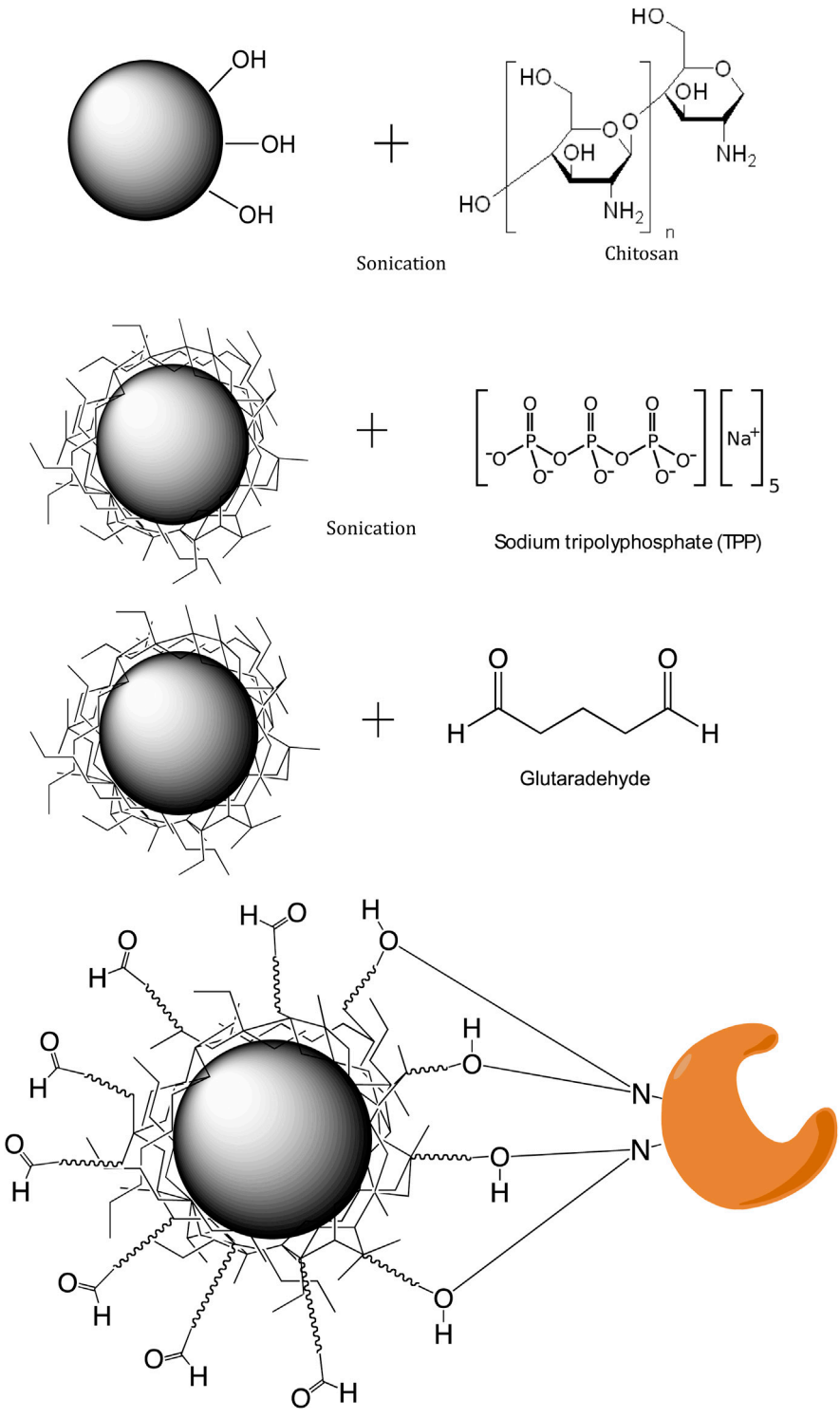

FIGURE 2
Schematic diagram of surface modification and enzyme immobilization.

2.6 Activity measurement

The activities of native exo-cellulase, endo-cellulase, β-glucosidase (βG), and their bioconjugates were measured using carboxymethyl cellulose (CMC) and cellobiose (CB) as substrates. The rate of reducing sugar production was determined by the 3,5-dinitrosalicylic acid (DNS) reducing sugar assay. CMC served as the substrate for exo-cellulase, endo-cellulase, and their bioconjugates, while CB was used for βG and its bioconjugate. The DNS reagent was prepared according to Ghose (1987)(Ghose, 1987). 1 mL of CMC or CB was placed in a heating block at 37°C. Native enzymes and bioconjugates were then added to the substrates and allowed to

react for 30 min. Following this, 1 mL of the reaction mixture was added to 1 mL of DNS reagent and heated in boiling water for 5 min. The optical density was measured at 540 nm using a spectrophotometer.

2.7 Optimum bioconjugates ratio assessment

The optimum ratio of bioconjugates to produce glucose was observed. Three different levels (100 μg, 200 μg, and 300 μg) of each bioconjugate were mixed and added to the CMC (2% (w/v)) and paper powder (2% (w/v)). Glucose production with seven different ratios of bioconjugate mixtures (exo-, endo-, βG: 111,112,113,121,131,211,311, the number represents mixing ratio, for instant, 111 represents 0.1 mg of each bioconjugate) of bioconjugates was monitored for 24 h using YSI 2007 biochemical analyzer.

2.8 Thermal stability

The thermal stabilities of native enzymes and bioconjugates were assessed by subjecting 1–2 mL of each sample to varying temperatures (45°C, 65°C, and 85°C) in a heating block. At hourly intervals, samples were removed from the heating block and mixed with substrates (CMC and cellulose powder). These reaction mixtures were then incubated at 45°C for 1 hour. Glucose production from each reaction mixture was subsequently quantified using a YSI 2007 biochemical analyzer.

2.9 Recycle stability

The recycling stability of CS-MNP bioconjugates, including Exo-CS-MNPs, Endo-CS-MNPs, and βG-CS-MNPs, was assessed by measuring glucose production from these bioconjugates over 20 consecutive cycles. To achieve this, CMC in citrate buffer served as the substrate. For each cycle, the bioconjugates were mixed with 1 mL of a 2% (w/v) CMC solution and incubated for 1 h at 45°C in a heating block to allow the reaction to proceed. After the reaction, the glucose concentration was determined using the YSI 2700 glucose analyzer. Following glucose measurement, the bioconjugates were collected by placing a magnet at the bottom of a 1.5 mL Eppendorf tube, causing the magnetic nanoparticles to aggregate at the tube's base. The CMC solution was then carefully removed using a syringe and transferred to a separate 45 mL tube for further analysis or disposal. To prepare the bioconjugates for the next cycle, they were washed with 1 mL of citrate buffer. The magnetic decantation process was repeated to ensure that the bioconjugates were thoroughly cleaned and ready for reuse. This process of reaction, measurement, collection, and washing was repeated for a total of 20 cycles, enabling the evaluation of the bioconjugates' stability and effectiveness in repeated uses. The consistency in glucose production across these cycles would indicate the robustness and durability of the bioconjugates in catalytic applications.

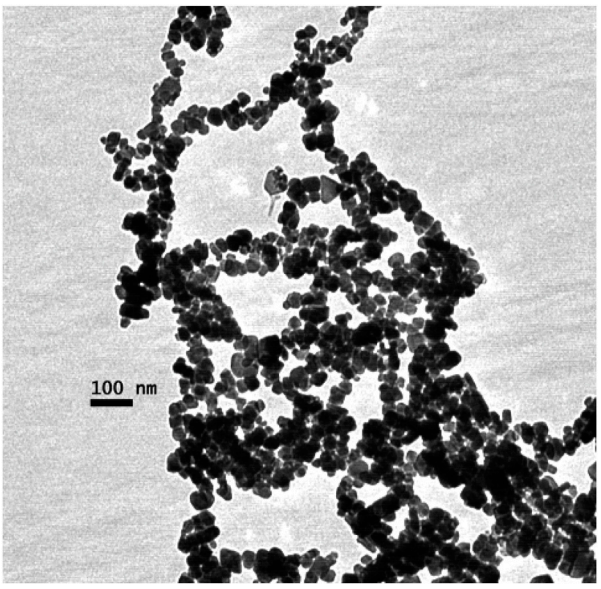

FIGURE 3
Transmission electron microscopy (TEM) images of Fe_3O_4 nanoparticles from oxidation of $Fe(OH)_2$.

2.10 Characterization

The Characterization process of MNPs and bioconjugates was similar methods used in previous research (Park et al., 2011; 2018) In brief, the size and morphology of fabricated MNPs were determined by Transmission Electron Microscopy (TEM, Hitachi H-7000) at 75 kV and BET. Samples for each step of the surface modifications on Endo-CS-MNPs were confirmed by surface analysis with X-ray Photoelectron Spectroscopy (XPS, 5,800 series, Multi-Technique ESCA systems). Survey and high resolution scans were collected and analyzed by XPSPeak 4.1 software to ensure their proper surface modifications.

3 Results and discussions

3.1 Particle size and physical properties of magnetic nanoparticles

A characteristic TEM image of synthesized MNPs shows a high degree of aggregation (Figure 3) which is explained by the strong magnetic dipole–dipole attractions feature between particles. This aggregation phenomenon for the MNPs is reported in other studies (Tan et al., 2018) it could also be related to the drying process of the samples prior to the morphological analyses. MNPs were spherical with an average diameter of 26 nm, as calculated from the BET analysis (Table 1). Although discrete nanoparticles of 26 nm in size were derived from BET method, the bulk of MNP preparations consisted of aggregated complexes of >140 nm in average size corroborated by dynamic light scattering and TEM results usually show higher aggregation causing solution drying effect on the specimen grids. The particle size was consistent with previously reported results

TABLE 1 Physical properties of magnetic nanoparticles from the $Fe(OH)_2$ oxidation method (A_S–surface area, D_{BET}–particle size based on BET, D_{TEM}–particle size based on TEM, M_S–saturation magnetization, D_{SOL}–particle size in solution-based on DLS).

Method	A_s (m^2 g^{-1})	D_{BET} (nm)	D_{TEM} (nm)	M_S (emu g^{-1})	D_{SOL} (nm)*
Bare MNPs	44 (±0.2)	26 (±0.1)	24 (±11)	62.3	140 (±25)

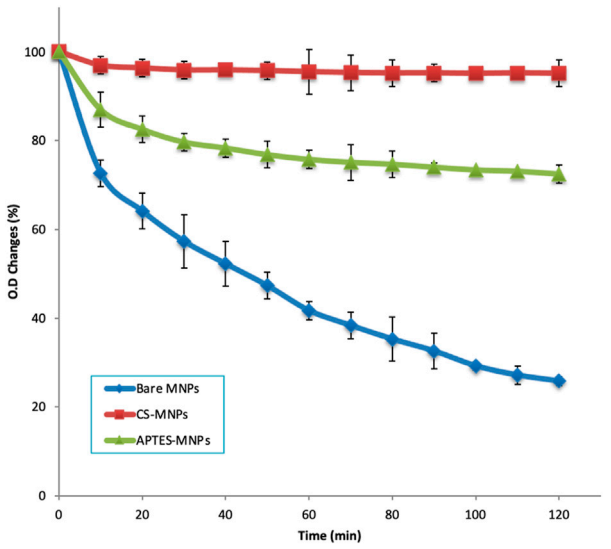

FIGURE 4
Particle settlement comparison: bare MNPs, APTES-MNPs, and CS-MNPs over 2 hours (particle concentration 0.025 mg/mL for all samples).

(Kouassi et al., 2005; Mürbe et al., 2008; Amstad et al., 2009; Amstad et al., 2009; Sillu and Agnihotri, 2020; Dong et al., 2024). The average size of the MNPs from TEM (D_{TEM}) analysis showed good agreement with BET results.

The saturated magnetization (M_S) of nanoparticles is an important measure of their magnetic strength under a fully saturated magnetic field., The Ms value is reported to be 62.3 emu/g, which aligns with data from Park et al. (2018). This is lower than the Ms of bulk magnetite, a phenomenon that is consistent with other studies (Hwang et al., 1997; Tada et al., 2003). The reduction in Ms for nanoparticles compared to bulk material can be attributed to two key factors: decreased particle size and increased surface area (Tada et al., 2003). The study also examines how surface modifications impact the stability of MNPs in solution over time. Three types of nanoparticles were evaluated: unmodified MNPs, APTES-modified MNPs (APTES-MNPs), and chitosan-modified MNPs (CS-MNPs). The results (Figure 4) are summarized as follows.

- CS-MNPs retained over 95% of their original optical density after 2 hours. This indicates excellent colloidal stability, which is crucial for applications like drug delivery or medical imaging, where nanoparticles need to remain dispersed for extended periods.
- APTES-MNPs showed around 72% retention of their initial optical density, meaning they are fairly stable but still subject to some degree of aggregation over time.
- Bare MNPs exhibited a significant decrease, losing 75% of their initial optical density within 2 hours. This rapid decline suggests that unmodified nanoparticles are prone to aggregation due to strong magnetic dipole-dipole interactions, which cause the particles to cluster together in the absence of surface stabilizers.

The findings imply that surface modification, particularly with materials like chitosan, can dramatically improve the colloidal stability of MNPs. Surface coatings reduce the magnetic interaction between particles and provide steric or electrostatic repulsion, preventing rapid aggregation. This enhancement of stability is particularly important for biomedical applications where nanoparticles need to maintain dispersion in biological fluids for effective performance.

3.2 Colloidal stability of different surface modification

Colloidal stability refers to a system's ability to keep particles dispersed without aggregating (Dobiáš, 1993). In conventional systems, stability is often explained by DLVO (Derjaguin-Landau-Verwey-Overbeek) theory, which considers the balance between attractive van der Waals forces (V_{vw}) and repulsive electrostatic forces (V_{ES}). However, for magnetic nanoparticles, this explanation is insufficient because MNPs have an additional magnetic dipole-dipole interaction (VM) due to their inherent magnetic properties. Thus, an extended or modified DLVO theory has been proposed to account for these magnetic interactions (Dobiáš, 1993; Elimelech et al., 1998; de Vicente et al., 2000). Surface modification of MNPs is a crucial strategy to improve their colloidal stability. By altering the surface chemistry, it's possible to change the balance of forces acting on the nanoparticles. In this study, two types of surface modifications, APTES and CS, were tested. Despite the fact that zeta potential values, which indicate the surface charge and are typically used as a measure of colloidal stability, were not significantly different between APTES-MNP (−20 mV ± 3.3) and CS-MNP (−19.3 mV ± 1.1), their settling behaviors showed notable differences. The DLS size measurements confirmed that the aggregation sizes for both types of modified particles were similar (140 nm), further supporting that there were no major differences in the forces described by DLVO theory (VvdW, VES, and VM). However, the fact that the two modified particles settled differently suggests that the buoyancy effect introduced by the surface modifications may be responsible for their different behaviors. This implies that surface modification alters not just electrostatic interactions but also other factors such as hydrodynamic forces or steric stabilization, which can influence colloidal stability in more subtle ways. The findings highlight the

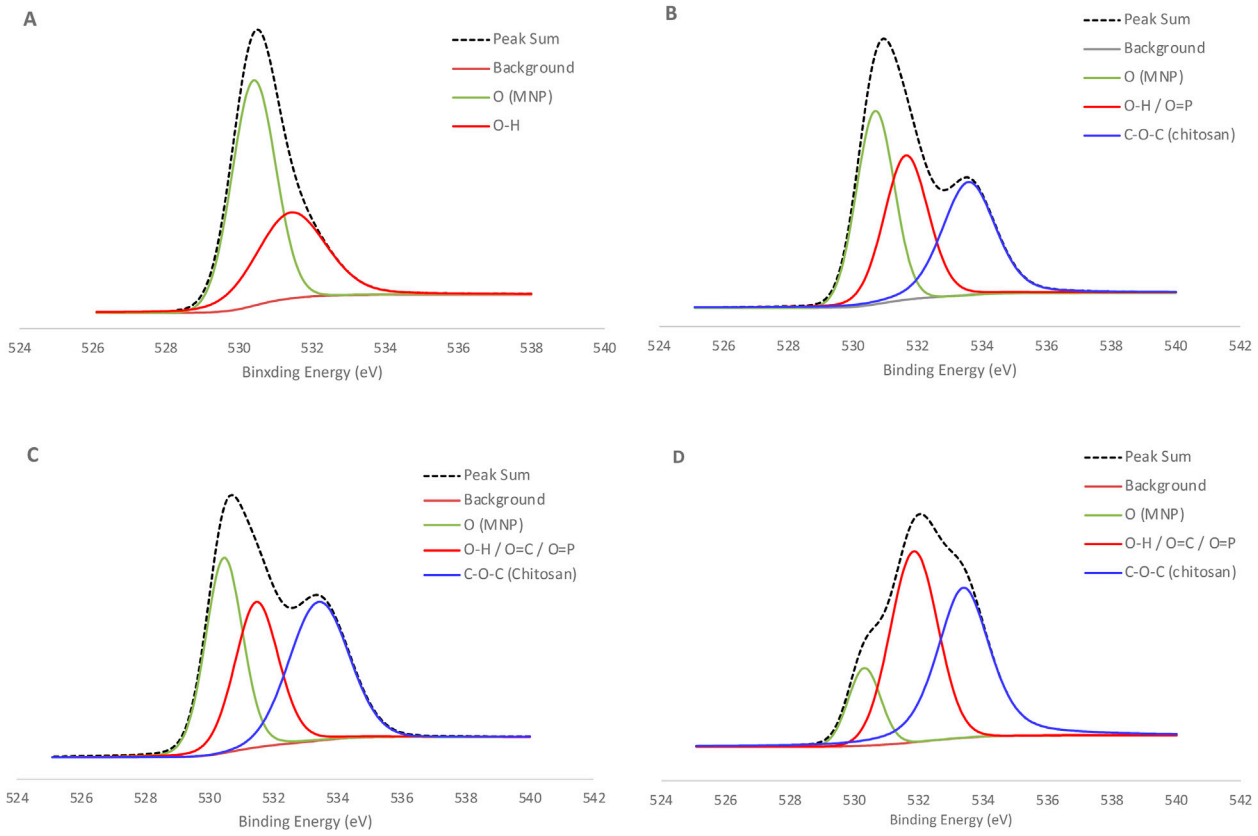

FIGURE 5
High resolution XPS spectra of O1s for each step of bioconjugate synthesis using Endo-CS-MNPs **(A)** Bare MNPs **(B)** CS-MNPs **(C)** CS-MNPs with Glutaraldehyde **(D)** Endo-cellulase-CS-MNPs.

complexity of colloidal stability in magnetic nanoparticles. While traditional metrics like zeta potential and aggregation size give useful insights, they may not capture all the relevant factors, particularly for modified surfaces. The buoyancy effect, for example, might play a more significant role than previously considered, and this warrants further investigation to fully understand how surface chemistry impacts the overall stability and performance of MNPs in various applications.

3.3 Binding confirmation and surface analysis

Throughout the fabrication process of Endo-CS-MNPs, we conducted X-ray photoelectron spectroscopy (XPS) to analyze and verify the chemical composition at each step. Specifically, we collected both survey spectra and high-resolution spectra focusing on the Fe2p1, C1s, O1s, N1s, P1s, and Si2p orbitals. These measurements were crucial for confirming the presence and proper bonding of elements, thus ensuring the successful creation of the bioconjugates. For the fabrication of Endo-APTES-MNPs, we employed a method involving APTES and glutaraldehyde for the immobilization process. Previous studies conducted by our research group demonstrated that this method effectively modified the nanoparticles, supporting the successful attachment of the desired functional groups (Park et al., 2011; 2018). The shift in the peak position of the high-resolution O1s spectra, as depicted in Figure 5, suggests a modification in the surface properties of the material. For

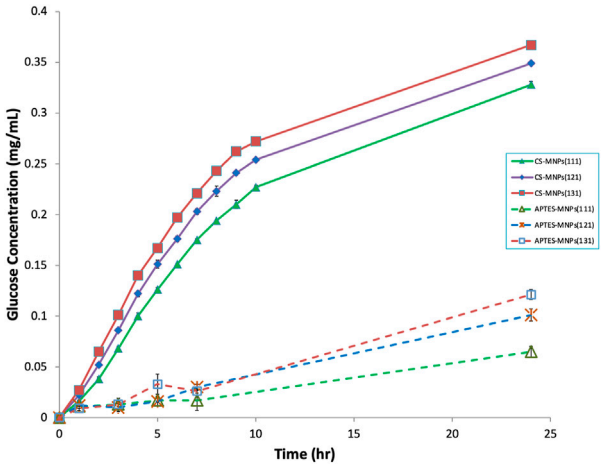

FIGURE 6
Glucose production with different ratio of exo-, endo-, and βG bioconjugates on CMC substrate. Number in the bracket represents the ration (exo, endo, βG).

TABLE 2 Protein binding efficiency, specific activity, and activity retention.

Sample ID	Binding Efficiency	Enzyme On MNPs	Specific Activity	Activity Retention
	(%)	(μg/mg)	(μg sugar/g protein)	(%)
Exo-APTES-MNPs	61.8%	447.9	71.6	13.9%
Endo-APTES-MNPs	47.8%	417.8	72.0	0.8%
βG-APTES-MNPs	8.7%	55.5	247.2	33.3%
Exo-CS-MNPs	65.5%	474.3	62.9	12.2%
Endo-CS-MNPs	48.7%	425.4	94.1	1.1%
βG-CS-MNPs	16.9%	88.4	218.0	29.4%

the bare MNPs, the most prominent peak was observed at a binding energy of 530.4 electron volts (eV). This value is characteristic of oxide crystal structures, indicating the presence of such structures on the surface of the MNPs (Kloprogge et al., 2006). Following the application of the chitosan coating, a significant peak was detected at 533.6 eV. This peak is attributed to the C-O-C bond present in chitosan. Additionally, there was a slight increase in intensity at 531.6 eV, which can be attributed to the presence of O=P and O-P bonds from sodium tripolyphosphate. When endo cellulase, an enzyme, binds to the magnetic nanoparticles, it induces notable shifts in the peaks. These shifts are caused by various functional groups within the protein structure of endo cellulase, specifically O-H, O-C, O=C, O-N, and O-C-N groups.

3.4 Characterization of bioconjugates

After immobilizing the enzymes onto MNPs, the amounts of residual protein (unbound) in the supernatant were measured to determine the levels of bound protein (binding efficiency). The specific activity of the immobilized enzymes was also measured to assess the activity loss during the immobilization process. Both the APTES + glutaraldehyde method and the CS + glutaraldehyde method showed no significant differences in binding efficiency and specific activity, indicating that both APTES and CS provided similar amounts of amine functional groups for the bi-functional glutaraldehyde to attach. The enzyme loading on MNPs of exo- and endo-cellulase was between 417 μg/mg and 417 μg/mg. This values is 6–7 times higher than the previous study (Kaur et al., 2023) However, β-glucosidase (βG) exhibited a relatively lower binding efficiency of 9%–17%, and these results align with earlier studies (Park et al., 2011; Park et al., 2018). The specific activities of bioconjugates are shown in Table 2. In particular, the activity retention of endo-cellulase in both APTES and CS coating bioconjugates was around 50% which is comparable to the previous study (Kaur et al., 2023). This diminished activity retention can be explained by the high native efficiency of endo-cellulase, which naturally produces substantial amounts of reducing sugars from carboxymethyl cellulose (CMC). The high baseline activity of the native enzyme establishes a difficult benchmark for its immobilized counterparts, making it challenging for bioconjugated enzymes to maintain or match the same level of enzymatic performance.

The absence of significant differences in binding efficiency and specific activity between the two methods emphasizes the versatility of both APTES and CS in providing functional groups necessary for effective immobilization. However, the variation in binding efficiency among the different enzymes—particularly the lower binding efficiency observed for β-glucosidase—raises important questions about the nature of enzyme-surface interactions. Factors such as enzyme size, structure, and the spatial arrangement of active sites likely play a role in determining how effectively an enzyme binds to a support surface. For β-glucosidase, its relatively lower binding efficiency could be a consequence of structural or steric hindrances that limit its attachment to the nanoparticle surface, compared to exo- and endo-cellulase.

3.5 Optimum bioconjugates ratio assessment

The study investigates the optimization of glucose production by combining three different levels of bioconjugates—exo-cellulase, endo-cellulase, and β-glucosidase (βG)—using two substrates: carboxymethyl cellulose (CMC) and cellulose powder. The goal was to determine the ideal ratio of these enzymes for maximizing glucose output. According to the findings, a higher concentration of endo-cellulase in the bioconjugate mix consistently resulted in better glucose production for both substrates. The bioconjugate mixture identified as "131," which incorporated both APTES-MNPs (and CS-MNPs, showed the most promising results, producing the highest glucose levels over a 24-h period (Figure 6). Specifically, with the CMC substrate, the CS-MNPs-based bioconjugate 131 mixture generated 0.367 mg/mL of glucose. In contrast, the APTES-MNPs-based bioconjugate 131 mixture produced significantly less glucose—just 33% of the amount produced by the CS-MNPs variant, yielding 0.121 mg/mL. The results reveal important insights into the catalytic efficacy of bioconjugates and the role of surface modifications in enzyme performance. The marked difference between the glucose production of CS-MNPs and APTES-MNPs highlights the critical influence that surface chemistry exerts on colloidal dispersion stability which we discussed from Figure 4. This suggests that surface modifications on magnetic nanoparticles can either amplify or limit the enzymatic efficiency, a key

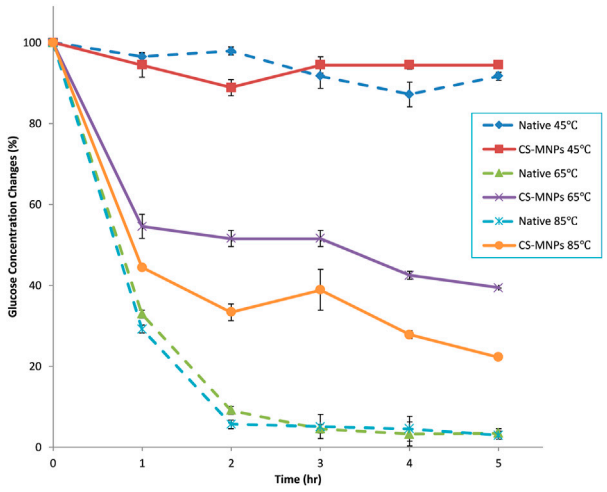

FIGURE 7
Thermal stability of native enzyme mixture and CS-MNPs bioconjugates mixture (131) at 45, 65 and 85 C.

consideration in industrial-scale applications where optimizing bioconversion rates is essential. The results also emphasize the importance of endo-cellulase in breaking down the internal bonds of cellulose, enhancing overall glucose yield. Most of previous studies used a cellulase mixture for immobilization on solid support and that leaves the enzyme ration unknown (Garcia et al., 1989; Tan et al., 2018; Sillu and Agnihotri, 2020; Paz-Cedeno et al., 2021; Zanuso et al., 2022; Kaur et al., 2023) In practical terms, the findings could be foundational in developing more efficient biocatalysts for biofuel production or other biotechnological processes that rely on cellulose degradation. By fine-tuning the enzyme ratios and nanoparticle modifications, industries could potentially achieve higher yields of glucose from lignocellulosic biomass, which is critical for sustainable energy production.

3.6 Thermal stability

The glucose production of both the native enzyme mixture and the bioconjugate mixture was analyzed at 45°C, 65°C, and 85°C to assess the thermal stability of immobilized enzymes. The underlying hypothesis is that the three-dimensional structures of immobilized enzymes are stabilized at elevated temperatures due to covalent multipoint attachment to solid supports. This structural reinforcement may provide greater resistance to thermal denaturation compared to their free counterparts. Previous research has demonstrated that native exo-, endo-cellulase, and β-glucosidase (βG) are highly sensitive to heat, particularly at temperatures exceeding 50°C (Andreaus et al., 1999). As depicted in Figure 7, the native enzyme mixture exhibits a dramatic decline in activity, losing more than 95% of its functionality within 2 hours at temperatures above 65°C. This rapid loss can be attributed to the unfolding of the enzyme's tertiary structure, a process accelerated by thermal stress. In contrast, the bioconjugates formed with chitosan-modified magnetic nanoparticles (CS-MNPs) showed a remarkable improvement in thermal stability. At 65°C, the bioconjugates retained 39.4% of their glucose production capacity, and even at the extreme temperature of 85°C, 22.2% of their initial activity was sustained after 5 hours.

This difference highlights the significant impact of immobilization on enzyme performance. The covalent attachment to the support not only anchors the enzymes but also prevents the excessive molecular flexibility that typically leads to denaturation under thermal stress. This stabilization offers substantial benefits in industrial applications, where processes often occur at elevated temperatures. Immobilized enzymes, such as the CS-MNP bioconjugates, demonstrate a more resilient structure, making them ideal for long-term use in harsh conditions, leading to both economic and practical advantages in enzymatic bioconversion processes.

3.7 Recycling stability and product accumulation

The glucose production resulting from the hydrolysis of carboxymethyl cellulose (CMC) by the CS-MNPs bioconjugate was assessed in each cycle, as shown in Figure 8A. Initially, the bioconjugate generated a glucose concentration of 0.039 mg/mL, which represents roughly 10% of the yield produced by the native enzyme. Remarkably, over 80% of this initial glucose output was maintained through the 10th cycle. However, after the 10th cycle, a noticeable decline in glucose concentration was observed, dropping to 33% (0.013 mg/mL) of the original value by the 20th cycle.

Figure 8B provides a comparative analysis of glucose productivity between native enzymes and bioconjugates when acting on CMC. While the native enzymes exhibited a glucose yield approximately ten times higher than that of the bioconjugates in the initial phase, the cumulative glucose production from the bioconjugates reached parity with the native enzyme by the 10th cycle. This data highlights a significant trade-off between initial efficiency and long-term sustainability in enzyme performance. The native enzyme's superior glucose production in the early stages emphasizes its high catalytic efficiency, a feature critical for processes that require rapid glucose output. In contrast, the bioconjugate, though initially lagging, demonstrates impressive stability over repeated cycles. The retention of 80% glucose production through 10 cycles suggests that the bioconjugate may be better suited for prolonged, repetitive use without substantial loss of activity. The decline in glucose production after the 10th cycle is a critical point for further discussion. It indicates that while bioconjugates offer extended utility, they are not immune to gradual deactivation or inhibition, likely due to enzyme denaturation, substrate fouling, or the depletion of active binding sites on the CS-MNPs surface. By the 20th cycle, the bioconjugate retains only 33% of its original glucose yield, reflecting a clear limitation for applications requiring sustained, high-level output over many cycles. Considering the fact that bioconjugates achieve cumulative productivity equivalent to native enzymes by the 10th cycle, it may offer a more sustainable and economically viable solution in processes where long-term performance and enzyme recyclability are essential.

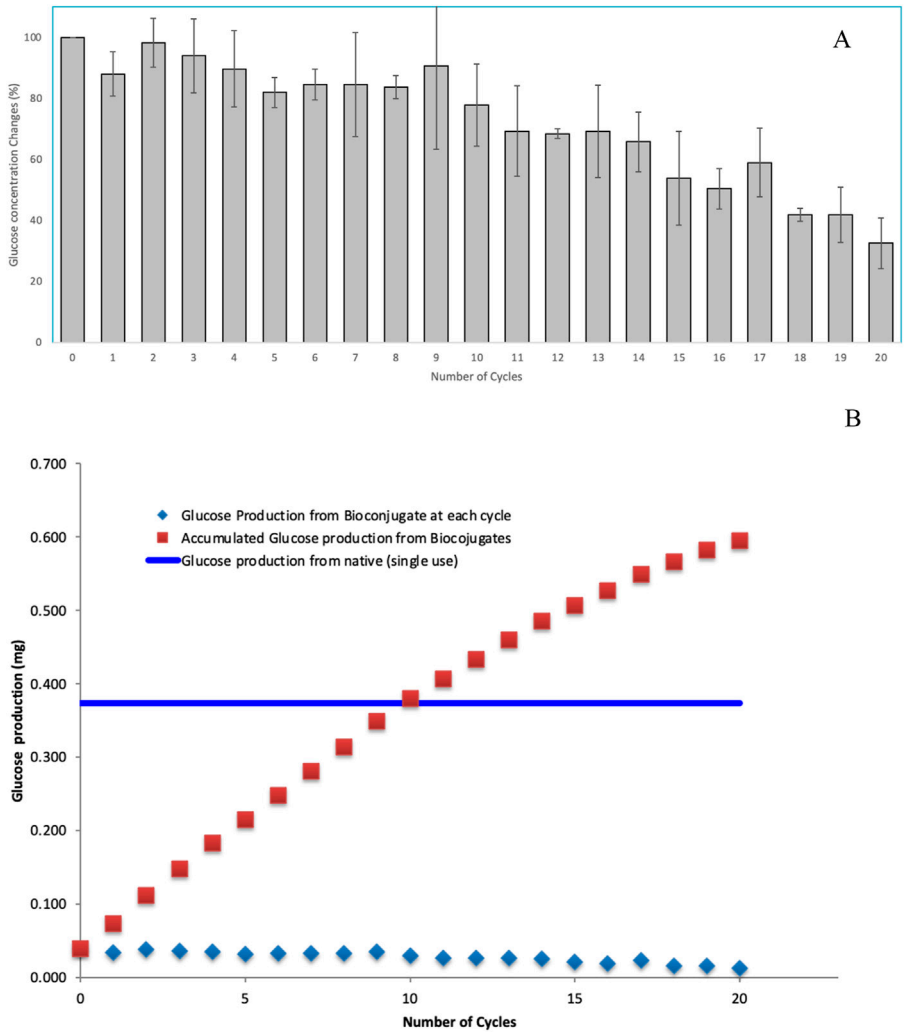

FIGURE 8
Recycle stability assessment by observing glucose production from hydrolysis of CMC for 20 consecutive cycles **(A)** and productivity comparison with native enzymes **(B)**.

4 Conclusion

In this study, we successfully immobilized three key cellulase enzymes—exo-cellulase, endo-cellulase, and β-glucosidase—on surface-modified magnetic nanoparticles (MNPs) using APTES (3-aminopropyltriethoxysilane) and chitosan (CS). This approach aimed to create a recyclable biocatalyst system for cellulose hydrolysis, with the broader goal of significantly reducing the costs associated with enzymatic hydrolysis, which is a critical bottleneck in biomass conversion processes. Through careful optimization, we controlled the MNP size to 26 nm using the $Fe(OH)_2$ oxidation method. This precise control over nanoparticle size was crucial to maximizing the enzyme binding efficiency and ensuring consistent catalytic activity. Two distinct surface modification strategies for MNPs were tested—one using APTES and the other using chitosan (CS)—to evaluate their colloidal stability and overall performance in enzyme immobilization. Our findings revealed that CS-modified MNPs displayed markedly superior colloidal stability compared to their APTES-modified counterparts, a critical factor in maintaining long-term activity and preventing enzyme aggregation. Glucose production experiments conducted with two substrates, carboxymethyl cellulose (CMC) and cellulose powder. CS-MNP bioconjugates exhibited approximately threefold higher glucose yields compared to APTES-MNP bioconjugates, highlighting the efficacy of CS as a surface modification agent in promoting enzyme-substrate interaction and catalytic efficiency. In addition to enhanced activity, CS-MNP bioconjugates demonstrated significantly improved thermal stability. While native enzymes experienced a sharp decline in glucose production above 65°C, with negligible activity remaining after 2 hours, the CS-MNP bioconjugates retained substantial activity under the same conditions. At 65°C, they preserved 39.4% of their productivity, and at 85°C, 22.2% over a 5-h period—demonstrating their resilience in high-temperature environments, which is a crucial advantage in industrial applications.

Moreover, the recyclability of CS-MNP bioconjugates was another significant advancement. In repeated use tests, they

maintained consistent glucose production over 20 cycles of cellulose hydrolysis. Remarkably, even after 10 cycles, the glucose yields from the CS-MNP bioconjugates remained comparable to those achieved with the single-use native enzymes. This recycling capability represents a major step forward in making enzymatic processes more sustainable and cost-effective. By maintaining high productivity while enabling enzyme reuse, this system opens new possibilities for large-scale cellulose degradation and biofuel production, offering not just a technical solution, but also a potential economic breakthrough in reducing the operational costs of industrial enzymatic hydrolysis.

Data availability statement

The original contributions presented in the study are included in the article/supplementary material, further inquiries can be directed to the corresponding author.

Author contributions

HP: Writing–original draft, Writing–review and editing, Funding, Conceptualization. PJ: Conceptualization, Funding acquisition, Investigation, Writing–review and editing, Supervision.

Funding

The author(s) declare that financial support was received for the research, authorship, and/or publication of this article. This research was supported by funding from the North Central Regional Sun Grant Center at South Dakota State University through a grant provided by the US Department of Transportation, Office of the Secretary, Grant No. DTOS59-07-G-00054. Additional funding was provided by the College of Arts, Science and Engineering (CASE) at the University of North Alabama.

Conflict of interest

The authors declare that the research was conducted in the absence of any commercial or financial relationships that could be construed as a potential conflict of interest.

Publisher's note

All claims expressed in this article are solely those of the authors and do not necessarily represent those of their affiliated organizations, or those of the publisher, the editors and the reviewers. Any product that may be evaluated in this article, or claim that may be made by its manufacturer, is not guaranteed or endorsed by the publisher.

References

Amorim, R. V. S., Melo, E. S., Carneiro-da-Cunha, M. G., Ledingham, W. M., and Campos-Takaki, G. M. (2003). Chitosan from Syncephalastrum racemosum used as a film support for lipase immobilization. *Bioresour. Technol.* 89, 35–39. doi:10.1016/S0960-8524(03)00035-X

Amstad, E., Zurcher, S., Mashaghi, A., Wong, J. Y., Textor, M., and Reimhult, E. (2009). Surface functionalization of single superparamagnetic iron oxide nanoparticles for targeted magnetic resonance imaging. *Small* 5, 1334–1342. doi:10.1002/smll.200801328

Andreaus, J., Azevedo, H., and Cavaco-Paulo, A. (1999). Effects of temperature on the cellulose binding ability of cellulase enzymes. *J. Mol. Catal. B Enzym.* 7, 233–239. doi:10.1016/S1381-1177(99)00032-6

Baniasadi, H., Ramazani, S. A. A., Mashayekhan, S., Farani, M. R., Ghaderinezhad, F., and Dabaghi, M. (2015). Design, fabrication, and characterization of novel porous conductive scaffolds for nerve tissue engineering. *Int. J. Polym. Mater. Polym. Biomaterials* 64, 969–977. doi:10.1080/00914037.2015.1038817

Barbosa, F. C., Silvello, M. A., and Goldbeck, R. (2020). Cellulase and oxidative enzymes: new approaches, challenges and perspectives on cellulose degradation for bioethanol production. *Biotechnol. Lett.* 42, 875–884. doi:10.1007/s10529-020-02875-4

de Vicente, J., Delgado, A. V., Plaza, R. C., Durán, J. D. G., and González-Caballero, F. (2000). Stability of cobalt ferrite colloidal particles. Effect of pH and applied magnetic fields. *Langmuir* 16, 7954–7961. doi:10.1021/la0003490

Dobiáš, B. (1993). *Coagulation and flocculation: theory and applications*. CRC Press.

Dong, L., Chen, G., Liu, G., Huang, X., Xu, X., Li, L., et al. (2024). A review on recent advances in the applications of composite Fe3O4 magnetic nanoparticles in the food industry. *Crit. Rev. Food Sci. Nutr.* 64, 1110–1138. doi:10.1080/10408398.2022.2113363

Elimelech, M., Jia, X., Gregory, J., and Williams, R. (1998). *Particle deposition and aggregation: measurement, modelling and simulation*. 1st Edn. Butterworth-Heinemann.

Elmi Fard, N., and Fazaeli, R. (2022). Fabrication of superhydrophobic 2/polyaniline/covalent organic frameworks/cotton fabric membrane and evaluation of its efficiency in separation of olive oil from water. *J. Chin. Chem. Soc.* 69, 2014–2026. doi:10.1002/jccs.202200368

Garcia, A., Oh, S., and Engler, C. R. (1989). Cellulase immobilization on Fe3O4 and characterization. *Biotechnol. Bioeng.* 33, 321–326. doi:10.1002/bit.260330311

Ghose, T. K. (1987). Measurement of cellulase activities. *Pure Appl. Chem.* 59, 257–268. doi:10.1351/pac198759020257

Godjevargova, T., Konsulov, V., and Dimov, A. (1999). Preparation of an ultrafiltration membrane from the copolymer of acrylonitrile-glycidylmethacrylate utilized for immobilization of glucose oxidase. *J. Membr. Sci.* 152, 235–240. doi:10.1016/S0376-7388(98)00222-1

Gomes, D., Rodrigues, A. C., Domingues, L., and Gama, M. (2015). Cellulase recycling in biorefineries—is it possible? *Appl. Microbiol. Biotechnol.* 99, 4131–4143. doi:10.1007/s00253-015-6535-z

Gomes, D. G., Serna-Loaiza, S., Cardona, C. A., Gama, M., and Domingues, L. (2018). Insights into the economic viability of cellulases recycling on bioethanol production from recycled paper sludge. *Bioresour. Technol.* 267, 347–355. doi:10.1016/j.biortech.2018.07.056

Gomes, D., Cunha, J., Zanuso, E., Teixeira, J., and Domingues, L. (2021). Strategies towards reduction of cellulases consumption: debottlenecking the economics of lignocellulosics valorization processes. *Polysaccharides* 2, 287–310. doi:10.3390/polysaccharides2020020

Gossuin, Y., Martin, E., Vuong, Q. L., Delroisse, J., Laurent, S., Stanicki, D., et al. (2022). Characterization of commercial iron oxide clusters with high transverse relaxivity. *J. Magnetic Reson. Open* 10–11, 100054. doi:10.1016/j.jmro.2022.100054

Guzmán, E., Llamas, S., Maestro, A., Fernández-Peña, L., Akanno, A., Miller, R., et al. (2016). Polymer–surfactant systems in bulk and at fluid interfaces. *Adv. Colloid Interface Sci.* 233, 38–64. doi:10.1016/j.cis.2015.11.001

Himmel, M. E., Ding, S.-Y., Johnson, D. K., Adney, W. S., Nimlos, M. R., Brady, J. W., et al. (2007). Biomass recalcitrance: engineering plants and enzymes for biofuels production. *Science* 315, 804–807. doi:10.1126/science.1137016

Horák, D., Babic, M., Macková, H., and Benes, M. J. (2007). Preparation and properties of magnetic nano- and microsized particles for biological and environmental separations. *J. Sep. Sci.* 30, 1751–1772. doi:10.1002/jssc.200700088

Hwang, J.-H., Dravid, V. P., Teng, M. H., Host, J. J., Elliott, B. R., Johnson, D. L., et al. (1997). Magnetic properties of graphitically encapsulated nickel nanocrystals. *J. Mater. Res.* 12, 1076–1082. doi:10.1557/JMR.1997.0150

Kaur, G., Taggar, M. S., and Kalia, A. (2023). Cellulase-immobilized chitosan-coated magnetic nanoparticles for saccharification of lignocellulosic biomass. *Environ. Sci. Pollut. Res.* 30, 111627–111647. doi:10.1007/s11356-023-27919-w

Kloprogge, J. T., Duong, L. V., Wood, B. J., and Frost, R. L. (2006). XPS study of the major minerals in bauxite: gibbsite, bayerite and (pseudo-)boehmite. *J. Colloid Interface Sci.* 296, 572–576. doi:10.1016/j.jcis.2005.09.054

Kouassi, G., Irudayaraj, J., and McCarty, G. (2005). Activity of glucose oxidase functionalized onto magnetic nanoparticles. *Biomagn. Res. Technol.* 3, 1. doi:10.1186/1477-044X-3-1

Kumar, A. (2000). A review chitin and chitosan applications, Reactive and Functional Polymers. *Int. J. Pattern Recognit. Artif. Intell.* 14, 1. Available at: http://www.worldscinet.com/ijprai/14/1401/S0218001400000027.html.(Accessed April 6, 2011).

Larnaudie, V., Ferrari, M. D., and Lareo, C. (2019). Techno-economic analysis of a liquid hot water pretreated switchgrass biorefinery: effect of solids loading and enzyme dosage on enzymatic hydrolysis. *Biomass Bioenergy* 130, 105394. doi:10.1016/j.biombioe.2019.105394

Liu, G., Zhang, J., and Bao, J. (2016). Cost evaluation of cellulase enzyme for industrial-scale cellulosic ethanol production based on rigorous Aspen Plus modeling. *Bioprocess Biosyst. Eng.* 39, 133–140. doi:10.1007/s00449-015-1497-1

Matusiak, J., Grządka, E., Maciołek, U., Godek, E., and Guzmán, E. (2022). The journey of tuning chitosan properties in colloidal systems: interactions with surfactants in the bulk and on the alumina surface. *Chem. Eng. J.* 450, 138145. doi:10.1016/j.cej.2022.138145

Michelin, M., Gomes, D. G., Romaní, A., Polizeli, M. de L. T. M., and Teixeira, J. A. (2020). Nanocellulose production: exploring the enzymatic route and residues of pulp and paper industry. *Molecules* 25, 3411. doi:10.3390/molecules25153411

Mo, H., Qiu, J., Yang, C., Zang, L., and Sakai, E. (2020). Preparation and characterization of magnetic polyporous biochar for cellulase immobilization by physical adsorption. *Cellulose* 27, 4963–4973. doi:10.1007/s10570-020-03125-6

Mohandes, F., Dehghani, H., Angizi, S., Ramedani, A., Dolatyar, B., Ramezani Farani, M., et al. (2022). Magneto-fluorescent contrast agents based on carbon Dots@Ferrite nanoparticles for tumor imaging. *J. Magnetism Magnetic Mater.* 561, 169686. doi:10.1016/j.jmmm.2022.169686

Mürbe, J., Rechtenbach, A., and Töpfer, J. (2008). Synthesis and physical characterization of magnetite nanoparticles for biomedical applications. *Mater. Chem. Phys.* 110, 426–433. doi:10.1016/j.matchemphys.2008.02.037

Nedylakova, M., Medinger, J., Mirabello, G., and Lattuada, M. (2024). Iron oxide magnetic aggregates: aspects of synthesis, computational approaches and applications. *Adv. Colloid Interface Sci.* 323, 103056. doi:10.1016/j.cis.2023.103056

Neeraj, G., Krishnan, S., Senthil Kumar, P., Shriaishvarya, K. R., and Vinoth Kumar, V. (2016). Performance study on sequestration of copper ions from contaminated water using newly synthesized high effective chitosan coated magnetic nanoparticles. *J. Mol. Liq.* 214, 335–346. doi:10.1016/j.molliq.2015.11.051

Paljevac, M., Primozic, M., Habulin, M., Novak, Z., and Knez, Z. (2007). Hydrolysis of carboxymethyl cellulose catalyzed by cellulase immobilized on silica gels at low and high pressures. *J. Supercrit. Fluids* 43, 74–80. doi:10.1016/j.supflu.2007.05.006

Papadaskalopoulou, C., Sotiropoulos, A., Novacovic, J., Barabouti, E., Mai, S., Malamis, D., et al. (2019). Comparative life cycle assessment of a waste to ethanol biorefinery system versus conventional waste management methods. *Resour. Conservation Recycl.* 149, 130–139. doi:10.1016/j.resconrec.2019.05.006

Park, H. J., McConnell, J. T., Boddohi, S., Kipper, M. J., and Johnson, P. A. (2011). Synthesis and characterization of enzyme-magnetic nanoparticle complexes: effect of size on activity and recovery. *Colloids Surfaces B Biointerfaces* 83, 198–203. doi:10.1016/j.colsurfb.2010.11.006

Park, H. J., Driscoll, A. J., and Johnson, P. A. (2018). The development and evaluation of β-glucosidase immobilized magnetic nanoparticles as recoverable biocatalysts. *Biochem. Eng. J.* 133, 66–73. doi:10.1016/j.bej.2018.01.017

Paz-Cedeno, F. R., Carceller, J. M., Iborra, S., Donato, R. K., Godoy, A. P., Veloso de Paula, A., et al. (2021). Magnetic graphene oxide as a platform for the immobilization of cellulases and xylanases: ultrastructural characterization and assessment of lignocellulosic biomass hydrolysis. *Renew. Energy* 164, 491–501. doi:10.1016/j.renene.2020.09.059

Pino, M. S., Rodríguez-Jasso, R. M., Michelin, M., and Ruiz, H. A. (2019). Enhancement and modeling of enzymatic hydrolysis on cellulose from agave bagasse hydrothermally pretreated in a horizontal bioreactor. *Carbohydr. Polym.* 211, 349–359. doi:10.1016/j.carbpol.2019.01.111

Ramezani Farani, M., Azarian, M., Heydari Sheikh Hossein, H., Abdolvahabi, Z., Mohammadi Abgarmi, Z., Moradi, A., et al. (2022). Folic acid-adorned curcumin-loaded iron oxide nanoparticles for cervical cancer. *ACS Appl. Bio Mater.* 5, 1305–1318. doi:10.1021/acsabm.1c01311

Ravi Kumar, M. N. V. (2000). A review of chitin and chitosan applications. *React. Funct. Polym.* 46, 1–27. doi:10.1016/S1381-5148(00)00038-9

Rezaei, B., Yari, P., Sanders, S. M., Wang, H., Chugh, V. K., Liang, S., et al. (2024). Magnetic nanoparticles: a review on synthesis, characterization, functionalization, and biomedical applications. *Small* 20, 2304848. doi:10.1002/smll.202304848

Sillu, D., and Agnihotri, S. (2020). Cellulase immobilization onto magnetic halloysite nanotubes: enhanced enzyme activity and stability with high cellulose saccharification. *ACS Sustain. Chem. Eng.* 8, 900–913. doi:10.1021/acssuschemeng.9b05400

Tada, M., Hatanaka, S., Sanbonsugi, H., Matsushita, N., and Abe, M. (2003). Method for synthesizing ferrite nanoparticles ~30 nm in diameter on neutral pH condition for biomedical applications. *J. Appl. Phys.* 93, 7566–7568. doi:10.1063/1.1558676

Tan, L., Tan, Z., Feng, H., and Qiu, J. (2018). Cellulose as a template to fabricate a cellulase-immobilized composite with high bioactivity and reusability. *New J. Chem.* 42, 1665–1672. doi:10.1039/C7NJ03271D

van Rijn, R., Nieves, I. U., Shanmugam, K. T., Ingram, L. O., and Vermerris, W. (2018). Techno-economic evaluation of cellulosic ethanol production based on pilot biorefinery data: a case study of sweet sorghum bagasse processed via L+SScF. *Bioenerg. Res.* 11, 414–425. doi:10.1007/s12155-018-9906-3

Vandani, S. A. K., Kalaee, M., Saravani, M. G., Fard, N. E., Rahmati, M., and Kamani, M. (2023). Preparation of magnetic Fe3O4/MoO3/MCM-22 photocatalyst and its study on metronidazole adsorption, degradation, and process optimization. *Russ. J. Phys. Chem.* 97, 618–632. doi:10.1134/S003602442304026X

Verma, C., Verma, D. K., Berdimurodov, E., Barsoum, I., Alfantazi, A., and Hussain, C. M. (2024). Green magnetic nanoparticles: a comprehensive review of recent progress in biomedical and environmental applications. *J. Mater Sci.* 59, 325–358. doi:10.1007/s10853-023-08914-5

Wen, F., Nair, N. U., and Zhao, H. (2009). Protein engineering in designing tailored enzymes and microorganisms for biofuels production. *Curr. Opin. Biotechnol.* 20, 412–419. doi:10.1016/j.copbio.2009.07.001

Zahn, D., Klein, K., Radon, P., Berkov, D., Erokhin, S., Nagel, E., et al. (2020). Investigation of magnetically driven passage of magnetic nanoparticles through eye tissues for magnetic drug targeting. *Nanotechnology* 31, 495101. doi:10.1088/1361-6528/abb0b4

Zanuso, E., Ruiz, H. A., Domingues, L., and Teixeira, J. A. (2022). Magnetic nanoparticles as support for cellulase immobilization strategy for enzymatic hydrolysis using hydrothermally pretreated corn cob biomass. *Bioenerg. Res.* 15, 1946–1957. doi:10.1007/s12155-021-10384-z